PERGAMON

International Journal of Solids and Structures 40 (2003) 6513–6526

INTERNATIONAL JOURNAL OF SOLIDS and STRUCTURES

www.elsevier.com/locate/ijsolstr

Singular electro-mechanical fields near the apex of a piezoelectric bonded wedge under antiplane shear

Chung De Chen, Ching Hwei Chue *

Department of Mechanical Engineering, National Cheng Kung University, Tainan 70101, Taiwan, ROC

Received 11 September 2002; received in revised form 9 June 2003

Abstract

This paper presents the explicit forms of singular electro-mechanical field in a piezoelectric bonded wedge subjected to antiplane shear loads. Based on the complex potential function associated with eigenfunction expansion method, the eigenvalue equations are derived analytically. Contrary to the anisotropic elastic bonded wedge, the results of this problem show that the singularity orders are single-root and may be complex. The stress intensity factors of electrical and mechanical fields are dependent. However, when the wedge angles are equal ($\alpha = \beta$), the orders become real and double-root. The real stress intensity factors of electrical and mechanical fields are then independent. The angular functions have been validated when they are compared with the results of several degenerated cases in open literatures.

Keywords: Piezoelectric; Wedge; Stress singularity; Eigenfunction expansion; Stress intensity factor

1. Introduction

Due to the electro-mechanical coupling behavior, piezoelectric materials (e.g. lead zirconate titanate (PZT)) are widely used in various application fields (Parton and Kudryavtsev, 1988; Gandhi and Thompson, 1992; Uchino, 1997). Several typical structures shown in Fig. 1 can be found in transducers, wave filters, sensors, resonators and actuators. The piezoelectric materials are bonded to composite materials, electrode thin film, or piezoelectric materials. The local region marked by dotted circle is considered as a wedge. Because of the discontinuities of material properties and geometry, the stresses at the apex of the wedge may go to infinite. Failures such as crack will initiate from that point since the piezoelectric material is brittle.

The singularity problems near the apex of isotropic or anisotropic wedge have been widely investigated (e.g. Bogy, 1968, 1971; Theocaris, 1974; Ma and Hour, 1989; Chen and Nisitani, 1992, 1993). The singular stress fields can be expressed as follows:

* Corresponding author. Tel.: +886-6-2757575x62165; fax: +886-6-2352973.
E-mail address: chchue@mail.ncku.edu.tw (C.H. Chue).

0020-7683/$ - see front matter © 2003 Elsevier Ltd. All rights reserved.
doi:10.1016/S0020-7683(03)00415-3

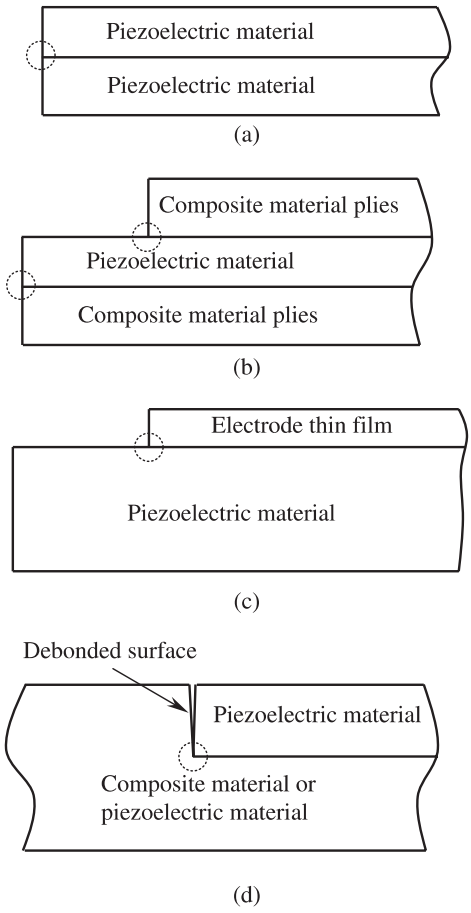

Fig. 1. Several typical wedge structures in actuators. (a) Piezoelectric–piezoelectric wedges; (b) piezoelectric–composite wedges; (c) piezoelectric–conductor wedges; (d) debonded junctions involving piezoelectric materials.

$$\sigma_{ij}(r,\theta) = K_{ij} r^{\lambda-1} f_{ij}(\theta) \tag{1}$$

where λ is the stress singularity orders, $f_{ij}(\theta)$ the angular function and K_{ij} the stress intensity factors. The order λ, which is obtained from the root of the determinant of the characteristic matrix, may be real or complex. If λ is a double root, the stresses near the apex of the wedge may exhibit logarithm-type singularity depending on the rank of the characteristic matrix (Dempsey and Sinclair, 1979). The factors K_{ij} may also be real or complex. Based on the Mellin transform or the eigenfunction expansion method, the order λ and the angular function f_{ij} are obtained analytically. However, the determination of the stress intensity factors is more complicated. It depends on the remote geometry and loading conditions and the numerical methods are required. For example, Munz and Yang (1993) employed the finite element method to compute the stress intensity factors when the singularity order and the angular functions are pre-determined analytically. In this approach, the angular functions play an important role because the validity of the computed intensity factors has to be examined for different angle θ.

It is known that the piezoelectric-elastic problems can be decoupled into inplane and antiplane problems if the poling axis is parallel or perpendicular to x–y plane (Fig. 2). The inplane problems of singular electromechanical fields near the apex of a bonded wedge have been solved when the poling axis is in x–y plane

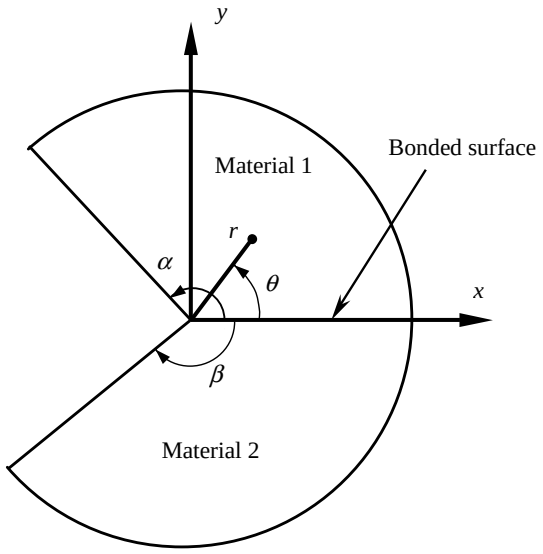

Fig. 2. Two-material bonded wedge.

(Xu and Rajapakse, 2000; Chue and Chen, 2002). Chue and Chen (2003) investigated the piezoelectric bonded wedge under various boundary conditions by using the Mellin transform. The poling axis is directed along z-axis and the antiplane shear stresses $(\tau_{\theta z},\tau_{rz})$ are coupled with the inplane electrical fields (D_r, D_θ).

Based on the complex functions and eigenfunction expansion, the singular electro-mechanical fields for a piezoelectric bonded wedge are analyzed in this study. The boundary conditions at both edges of wedge are traction free and electrically insulated. It is a specific case in Chue and Chen (2003). However, Chue and Chen (2003) only derived the antiplane stress singularity orders and the singular electro-mechanical fields near the apex of the wedge were not included. Two cases with $\alpha = \beta$ and $\alpha \neq \beta$ are discussed separately in this study. Most emphasis is placed on the intensity factors, angular functions and the conditions that the antiplane singularity order is complex. The results are different from the case of an anisotropic bonded wedge under antiplane shear (Ma and Hour, 1989), in which the orders are always real.

2. Basic formulations

The constitutive equation for antiplane field of a piezoelectric medium is given as follows

$$\begin{Bmatrix} \tau_{\theta z} \\ \tau_{rz} \\ D_r \\ D_\theta \end{Bmatrix} = \begin{bmatrix} C_{44} & 0 & 0 & -e_{15} \\ 0 & C_{44} & -e_{15} & 0 \\ 0 & e_{15} & \varepsilon_{11} & 0 \\ e_{15} & 0 & 0 & \varepsilon_{11} \end{bmatrix} \begin{Bmatrix} \gamma_{\theta z} \\ \gamma_{rz} \\ E_r \\ E_\theta \end{Bmatrix} \tag{2}$$

where $(\tau_{\theta z}, \tau_{rz})$ are the shear stresses, $(\gamma_{\theta z}, \gamma_{rz})$ the shear strains, (D_r, D_θ) the electric displacement, (E_r, E_θ) the electric field strength, C_{44} the elastic modulus at constant electric field, e_{15} the piezoelectric constant, and ε_{11} the dielectric permitivity at constant strains. The static equilibrium equations and Maxwell's equation under electro-static condition are given as

$$\frac{\partial}{\partial r}(r\tau_{rz}) + \frac{\partial \tau_{\theta z}}{\partial \theta} = 0 \tag{3a}$$

$$\frac{\partial}{\partial r}(rD_r) + \frac{\partial D_\theta}{\partial \theta} = 0 \tag{3b}$$

The strain–displacement and electric field–electric potential relations are as follows:

$$\gamma_{rz} = \frac{\partial w}{\partial r}, \quad \gamma_{\theta z} = \frac{1}{r}\frac{\partial w}{\partial \theta}, \quad E_r = -\frac{\partial \Phi}{\partial r}, \quad E_\theta = -\frac{1}{r}\frac{\partial \Phi}{\partial \theta} \tag{4}$$

where w and Φ are the displacement and electric potential, respectively. Combination of Eqs. (2)–(4) yields

$$C_{44}\nabla^2 w - e_{15}\nabla^2 \Phi = 0 \tag{5a}$$

$$e_{15}\nabla^2 w + \varepsilon_{11}\nabla^2 \Phi = 0 \tag{5b}$$

where $\nabla^2 = \partial^2/\partial r^2 + (1/r)\partial/\partial r + (1/r^2)\partial^2/\partial \theta^2$ is the Laplacian operator in polar coordinates. Define two analytical complex functions Ψ and ϕ related to w and Φ as

$$w = \mathrm{Re}[\Psi(z)] \tag{6a}$$

$$\Phi = \mathrm{Re}[\phi(z)] \tag{6b}$$

where $z = re^{i\theta}$. It is noted that Eq. (6) satisfies Eq. (5) automatically. In the eigenfunction expansion method, the complex functions are expressed as

$$\Psi = b_1 r^\lambda e^{i\lambda\theta} + b_2 r^{\bar{\lambda}} e^{i\bar{\lambda}\theta} \tag{7a}$$

$$\phi = b_3 r^\lambda e^{i\lambda\theta} + b_4 r^{\bar{\lambda}} e^{i\bar{\lambda}\theta} \tag{7b}$$

where $b_i (i = 1, \ldots, 4)$ are undetermined complex constants. The constant λ is the eigenvalue. Combination of Eqs. (2), (4), (6) and (7) yields

$$w = \mathrm{Re}[r^\lambda (c_1 \cos(\lambda\theta) + c_2 \sin(\lambda\theta))] \tag{8a}$$

$$\Phi = \mathrm{Re}[r^\lambda (c_3 \cos(\lambda\theta) + c_4 \sin(\lambda\theta))] \tag{8b}$$

$$\tau_{\theta z} = \mathrm{Re}[\lambda r^{\lambda-1}(C_{44}c_2 \cos(\lambda\theta) - C_{44}c_1 \sin(\lambda\theta) + e_{15}c_4 \cos(\lambda\theta) - e_{15}c_3 \sin(\lambda\theta))] \tag{8c}$$

$$\tau_{rz} = \mathrm{Re}[\lambda r^{\lambda-1}(C_{44}c_1 \cos(\lambda\theta) + C_{44}c_2 \sin(\lambda\theta) + e_{15}c_3 \cos(\lambda\theta) + e_{15}c_4 \sin(\lambda\theta))] \tag{8d}$$

$$D_\theta = \mathrm{Re}[\lambda r^{\lambda-1}(e_{15}c_2 \cos(\lambda\theta) - e_{15}c_1 \sin(\lambda\theta) - \varepsilon_{11}c_4 \cos(\lambda\theta) + \varepsilon_{11}c_3 \sin(\lambda\theta))] \tag{8e}$$

$$D_r = \mathrm{Re}[\lambda r^{\lambda-1}(e_{15}c_1 \cos(\lambda\theta) + e_{15}c_2 \sin(\lambda\theta) - \varepsilon_{11}c_3 \cos(\lambda\theta) - \varepsilon_{11}c_4 \sin(\lambda\theta))] \tag{8f}$$

$$E_\theta = -\mathrm{Re}[\lambda r^{\lambda-1}(c_4 \cos(\lambda\theta) - c_3 \sin(\lambda\theta))] \tag{8g}$$

$$E_r = -\mathrm{Re}[\lambda r^{\lambda-1}(c_3 \cos(\lambda\theta) + c_4 \sin(\lambda\theta))] \tag{8h}$$

where $c_1 = b_1 + \bar{b}_2$, $c_2 = i(b_1 - \bar{b}_2)$, $c_3 = b_3 + \bar{b}_4$, and $c_4 = i(b_3 - \bar{b}_4)$.

3. Dissimilar piezoelectric bonded wedge

Consider a two-bonded piezoelectric wedge as shown in Fig. 2. The wedge angles of piezoelectric materials 1 and 2 are denoted as α and β, respectively. Let the bonded interface be x-axis. The conditions at the boundary edges are assumed to be free of traction and electrically insulated:

$$\tau_{\theta z}^{(1)}(r,\alpha) = \tau_{\theta z}^{(2)}(r,-\beta) = D_{\theta}^{(1)}(r,\alpha) = D_{\theta}^{(2)}(r,-\beta) = 0 \tag{9}$$

The continuity conditions at the bonded interface are

$$\begin{aligned} &\tau_{\theta z}^{(1)}(r,0) = \tau_{\theta z}^{(2)}(r,0), \quad w^{(1)}(r,0) = w^{(2)}(r,0), \\ &D_{\theta}^{(1)}(r,0) = D_{\theta}^{(2)}(r,0), \quad E_{r}^{(1)}(r,0) = E_{r}^{(2)}(r,0) \end{aligned} \tag{10}$$

The superscripts 1 and 2 in Eqs. (9) and (10) denote the materials 1 and 2, respectively. Substituting Eq. (8) into Eqs. (9) and (10), it gives an 8×8 homogeneous system as follows:

$$[M]\{X\} = \{0\} \tag{11}$$

where $\{X\} = [c_1^{(1)}, c_2^{(1)}, c_3^{(1)}, c_4^{(1)}, c_1^{(2)}, c_2^{(2)}, c_3^{(2)}, c_4^{(2)}]^{\mathrm{T}}$. The 8×8 matrix $[M]$ is composed of the coefficients of $c_2^{(1)}$ to $c_4^{(2)}$. It is function of the eigenvalue λ, the wedge angles, and the material properties. Two cases of $\alpha = \beta$ and $\alpha \neq \beta$ are considered here to determine the singular electro-mechanical field.

3.1. Equal wedge angles ($\alpha = \beta$)

Substituting $\beta = \alpha$ in $\det[M] = 0$, the characteristic equation becomes:

$$\sin^2(2\alpha\lambda) = 0 \tag{12}$$

Since $\sin^2(\alpha\lambda) \neq 0$ under the restrictions of $0 < \mathrm{Re}[\lambda] < 1$ and $0 < \alpha \leqslant \pi$, Eq. (12) can be rewritten as

$$\cos^2(\alpha\lambda) = 0 \tag{13}$$

It is seen that λ is always real and a double-root. By using Eq. (13), we find that the rank of the characteristic matrix $[M]$ is 6. Then the singularity is $r^{\lambda-1}$ type (Dempsey and Sinclair, 1979). There are two independent constants in Eq. (11), say $c_2^{(1)}$ and $c_4^{(1)}$. The other constants related to $c_2^{(1)}$ and $c_4^{(1)}$ are as follows

$$c_2^{(2)} = -\frac{a_{48}}{a_{26}a_{48} - a_{28}a_{46}} c_2^{(1)} + \frac{a_{28}}{a_{26}a_{48} - a_{28}a_{46}} c_4^{(1)} \tag{14a}$$

$$c_4^{(2)} = \frac{a_{46}}{a_{26}a_{48} - a_{28}a_{46}} c_2^{(1)} - \frac{a_{26}}{a_{26}a_{48} - a_{28}a_{46}} c_4^{(1)} \tag{14b}$$

$$c_1^{(1)} = c_3^{(1)} = c_1^{(2)} = c_3^{(2)} = 0 \tag{14c}$$

where

$$a_{26} = -\frac{e_{15}^{(1)} e_{15}^{(2)} + C_{44}^{(2)} \varepsilon_{11}^{(1)}}{e_{15}^{(1)} e_{15}^{(1)} + C_{44}^{(1)} \varepsilon_{11}^{(1)}} \tag{15a}$$

$$a_{28} = -\frac{e_{15}^{(2)} \varepsilon_{11}^{(1)} - e_{15}^{(1)} \varepsilon_{11}^{(2)}}{e_{15}^{(1)} e_{15}^{(1)} + C_{44}^{(1)} \varepsilon_{11}^{(1)}} \tag{15b}$$

$$a_{46} = -\frac{C_{44}^{(2)} e_{15}^{(1)} - C_{44}^{(1)} e_{15}^{(2)}}{e_{15}^{(1)} e_{15}^{(1)} + C_{44}^{(1)} \varepsilon_{11}^{(1)}} \tag{15c}$$

$$a_{48} = -\frac{e_{15}^{(1)} e_{15}^{(2)} + C_{44}^{(1)} \varepsilon_{11}^{(2)}}{e_{15}^{(1)} e_{15}^{(1)} + C_{44}^{(1)} \varepsilon_{11}^{(1)}} \tag{15d}$$

Substituting Eq. (14) into Eq. (8), the stresses and electric displacements can be expressed in the forms:

$$\tau_{\theta z} = K^{\sigma} r^{\lambda-1} \cos(\lambda\theta) \tag{16a}$$

$$\tau_{rz} = K^{\sigma} r^{\lambda-1} \sin(\lambda\theta) \tag{16b}$$

$$D_{\theta} = K^{D} r^{\lambda-1} \cos(\lambda\theta) \tag{16c}$$

$$D_{r} = K^{D} r^{\lambda-1} \sin(\lambda\theta) \tag{16d}$$

where K^{σ} and K^{D} are called the generalized stress and electric displacement intensity factors, respectively. They are defined as

$$K^{\sigma} = \lambda\left(C_{44}^{(1)} c_2^{(1)} + e_{15}^{(1)} c_4^{(1)}\right) \tag{17a}$$

$$K^{D} = \lambda\left(e_{15}^{(1)} c_2^{(1)} - \varepsilon_{11}^{(1)} c_4^{(1)}\right) \tag{17b}$$

For an interface crack, i.e. $\alpha = \beta = \pi$, the stress singularity order is $\mathrm{Re}[\lambda - 1] = -0.5$ and the angular functions are $\cos(\theta/2)$ and $\sin(\theta/2)$. The results are consistent with previous studies (e.g., Pak, 1990; Li and Fan, 2000).

Eq. (13) can be applied in the case of one material wedge. The singular electro-elastical fields and intensity factors are Eqs. (16) and (17) with dropping the superscript 1.

3.2. Unequal wedge angles $\alpha \neq \beta$

In this section, we consider the case of dissimilar piezoelectric bonded wedge with $\beta \neq \alpha$. Here we exclude the condition that $\alpha = 0$ or $\beta = 0$, which is equivalent to the case that one material wedge discussed in the above section. After elementary row operations on Eq. (11), it becomes

$$\begin{bmatrix} 1 & 0 & 0 & 0 & 0 & 0 & 0 & -M/(Q_c N) \\ 0 & 1 & 0 & 0 & 0 & 0 & 0 & -1/(Q_c N) \\ 0 & 0 & 1 & 0 & 0 & 0 & 0 & -M/N \\ 0 & 0 & 0 & 1 & 0 & 0 & 0 & -1/N \\ 0 & 0 & 0 & 0 & 1 & 0 & 0 & -M/(Q_c N) \\ 0 & 0 & 0 & 0 & 0 & 1 & 0 & -1/Q_c \\ 0 & 0 & 0 & 0 & 0 & 0 & 1 & -M/N \\ 0 & 0 & 0 & 0 & 0 & 0 & 0 & 1/(Q_e N) - 1/(Q_c N) \end{bmatrix} \begin{Bmatrix} c_1^{(1)} \\ c_2^{(1)} \\ c_3^{(1)} \\ c_4^{(1)} \\ c_1^{(2)} \\ c_2^{(2)} \\ c_3^{(2)} \\ c_4^{(2)} \end{Bmatrix} = \begin{Bmatrix} 0 \\ 0 \\ 0 \\ 0 \\ 0 \\ 0 \\ 0 \\ 0 \end{Bmatrix} \tag{18}$$

where

$$Q_c = -\frac{C_{44}^{(1)} \sin(\lambda\alpha)\cos(\lambda\beta) + C_{44}^{(2)} \cos(\lambda\alpha)\sin(\lambda\beta)}{e_{15}^{(1)} \sin(\lambda\alpha)\cos(\lambda\beta) + e_{15}^{(2)} \cos(\lambda\alpha)\sin(\lambda\beta)} \tag{19a}$$

$$Q_\varepsilon = \frac{e_{15}^{(1)} \sin(\lambda\alpha)\cos(\lambda\beta) + e_{15}^{(2)} \cos(\lambda\alpha)\sin(\lambda\beta)}{\varepsilon_{11}^{(1)} \sin(\lambda\alpha)\cos(\lambda\beta) + \varepsilon_{15}^{(2)} \cos(\lambda\alpha)\sin(\lambda\beta)} \tag{19b}$$

$$M = \frac{\cos(\lambda\alpha)}{\sin(\lambda\alpha)} \tag{19c}$$

$$N = -\frac{\cos(\lambda\alpha)\sin(\lambda\beta)}{\sin(\lambda\alpha)\cos(\lambda\beta)} \tag{19d}$$

In the derivation of Eq. (18), we have used the conditions $\alpha \neq \beta$ and $e_{15} \neq 0$. Consequently, Q_c and Q_ε cannot be zero. For nontrivial solution, it requires that

$$Q_c = Q_\varepsilon \equiv Q \tag{20}$$

Substituting Eq. (19) into Eq. (20), we obtain the characteristic equation

$$R_1 \sin^2[(\alpha-\beta)\lambda] + \sin^2[(\alpha+\beta)\lambda] - R_2 \sin[(\alpha+\beta)\lambda]\sin[(\alpha-\beta)\lambda] = 0 \tag{21}$$

where

$$R_1 = \frac{B_{11} + B_{22} - B_{12} - B_{21}}{B_{11} + B_{22} + B_{12} + B_{21}} \tag{22a}$$

$$R_2 = \frac{2B_{22} - 2B_{11}}{B_{11} + B_{22} + B_{12} + B_{21}} \tag{22b}$$

with

$$B_{11} = e_{15}^{(1)} e_{15}^{(1)} + \varepsilon_{11}^{(1)} C_{44}^{(1)} \tag{23a}$$

$$B_{12} = e_{15}^{(1)} e_{15}^{(2)} + \varepsilon_{11}^{(1)} C_{44}^{(2)} \tag{23b}$$

$$B_{21} = e_{15}^{(2)} e_{15}^{(1)} + \varepsilon_{11}^{(2)} C_{44}^{(1)} \tag{23c}$$

$$B_{22} = e_{15}^{(2)} e_{15}^{(2)} + \varepsilon_{11}^{(2)} C_{44}^{(2)} \tag{23d}$$

Eqs. (21)–(23) are exactly the same as Chue and Chen (2003), in which the Mellin transform was used. Since the rank of $[M]$ in Eq. (18) is 7, it is a $r^{\lambda-1}$ type singularity (Dempsey and Sinclair, 1979). Eq. (21) can be rewritten into the following two equations:

$$\sin[(\alpha+\beta)\lambda] + A_1 \sin[(\alpha-\beta)\lambda] = 0 \tag{24a}$$

$$\sin[(\alpha+\beta)\lambda] + A_2 \sin[(\alpha-\beta)\lambda] = 0 \tag{24b}$$

where

$$A_1 = -\frac{R_2 + \sqrt{R_2^2 - 4R_1}}{2}, \quad A_2 = -\frac{R_2 - \sqrt{R_2^2 - 4R_1}}{2} \tag{25}$$

The constants A_1 and A_2 are functions of the material properties and may be complex depending on $(R_2^2 - 4R_1)$. Thus, the eigenvalues λ may be complex, i.e., if $R_2^2 - 4R_1 \geqslant 0$, then λ is real; otherwise λ is complex. This is quite different from the anisotropic bonded wedge subjected to antiplane shear, in which the singularity orders are always real (Ma and Hour, 1989).

In the following, two cases of real and complex eigenvalues are discussed. The materials used are three typical piezo-ceramics, say PZT-4, PZT-5 and PZT-19. Their material properties are (Berlincourt et al., 1964; Parton and Kudryavtsev, 1988):

PZT-4: $C_{44} = 25.6 \times 10^9$ N/m^2, $e_{15} = 12.7$ C/N, $\varepsilon_{11} = 6.46 \times 10^{-9}$ F/m
PZT-5: $C_{44} = 21.1 \times 10^9$ N/m^2, $e_{15} = 12.3$ C/N, $\varepsilon_{11} = 8.11 \times 10^{-9}$ F/m
PZT-19: $C_{44} = 24.9 \times 10^9$ N/m^2, $e_{15} = 9.45$ C/N, $\varepsilon_{11} = 7.257 \times 10^{-9}$ F/m

3.2.1. Case (1): Real eigenvalues λ

Consider an example of a PZT-4–PZT-5 bonded wedge that the factor $(R_2^2 - 4R_1) = 0.0223035 > 0$. The eigenvalues are real. Fig. 3 plots the contours of the strongest singularity order at different wedge angles α and β. The orders are close to -0.5 when $\alpha + \beta = 360°$, i.e. the bonded wedge forms an interface crack. In addition, the singularity disappears in a region with $\alpha + \beta \leqq 180°$.

Since the rank of $[M]$ is 7, only one, say $c_2^{(1)}$, left undetermined for the eight unknown constants $c_1^{(1)}$ to $c_4^{(2)}$.

Define the generalized stress and electrical intensity factors K^σ and K^D as follows:

$$K^\sigma = \lambda\left(C_{44}^{(1)} + e_{15}^{(1)}Q\right)c_2^{(1)}, \quad K^D = \frac{\left(e_{15}^{(1)} - \varepsilon_{11}^{(1)}Q\right)K^\sigma}{C_{44}^{(1)} + e_{15}^{(1)}Q} \tag{26}$$

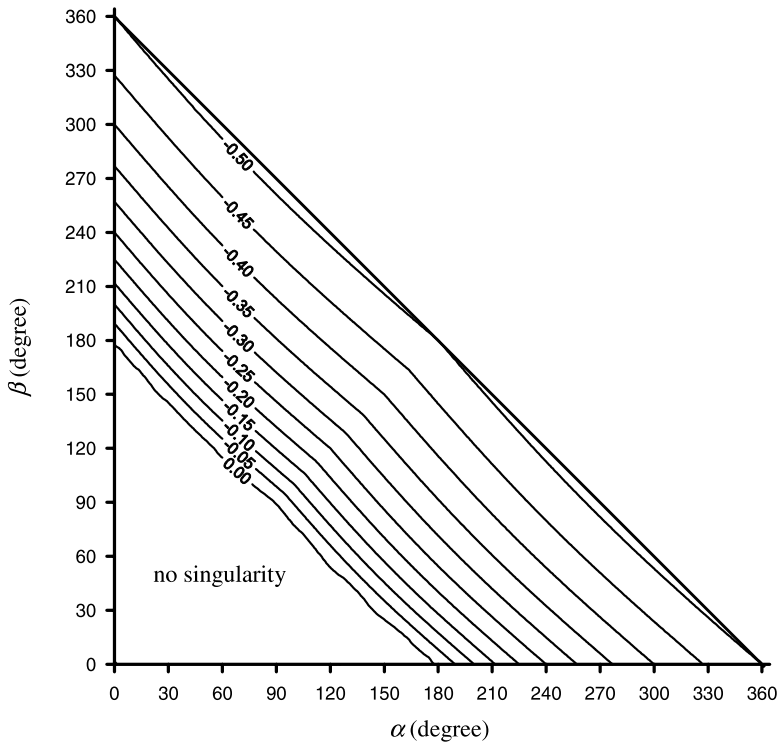

Fig. 3. The variation of the strongest singularity order of PZT-4–PZT-5 bonded wedges versus the wedge angles α and β.

The stresses and electric displacements can be derived as

$$\begin{aligned} \tau_{\theta z} &= K^{\sigma} r^{\lambda-1} f_{\theta z}(\theta), \quad \tau_{rz} = K^{\sigma} r^{\lambda-1} f_{rz}(\theta) \\ D_{\theta} &= K^{D} r^{\lambda-1} g_{\theta}(\theta), \quad D_{r} = K^{D} r^{\lambda-1} g_{r}(\theta) \end{aligned} \tag{27}$$

where $f_{\theta z}(\theta)$, $f_{rz}(\theta)$, $g_{\theta}(\theta)$ and $g_r(\theta)$ are the angular function for stresses and electrical displacements fields. They can be written as:

$$f_{\theta z}(\theta) = g_{\theta}(\theta) = \begin{cases} \cos(\lambda\theta) - \dfrac{\cos(\lambda\alpha)}{\sin(\lambda\alpha)} \sin(\lambda\theta) & \text{for material 1} \\ \cos(\lambda\theta) + \dfrac{\cos(\lambda\beta)}{\sin(\lambda\beta)} \sin(\lambda\theta) & \text{for material 2} \end{cases} \tag{28}$$

$$f_{rz}(\theta) = g_{r}(\theta) = \begin{cases} \sin(\lambda\theta) + \dfrac{\cos(\lambda\alpha)}{\sin(\lambda\alpha)} \cos(\lambda\theta) & \text{for material 1} \\ \sin(\lambda\theta) - \dfrac{\cos(\lambda\beta)}{\sin(\lambda\beta)} \cos(\lambda\theta) & \text{for material 2} \end{cases} \tag{29}$$

Fig. 4 plots the angular functions of a PZT-4–PZT-5 bonded wedge with $\alpha = 90°$ and $\beta = 180°$. The strongest singularity order $\mathrm{Re}[\lambda_1 - 1]$ is -0.347478. According to the boundary conditions (Eq. (9)) and continuity conditions (Eq. (10)), the angular functions $f_{\theta z}(\theta)$, and $g_{\theta}(\theta)$ are continuous along the bonded interface $\theta = 0°$ and vanish at the boundary edges $\theta = 90°$ and $-180°$.

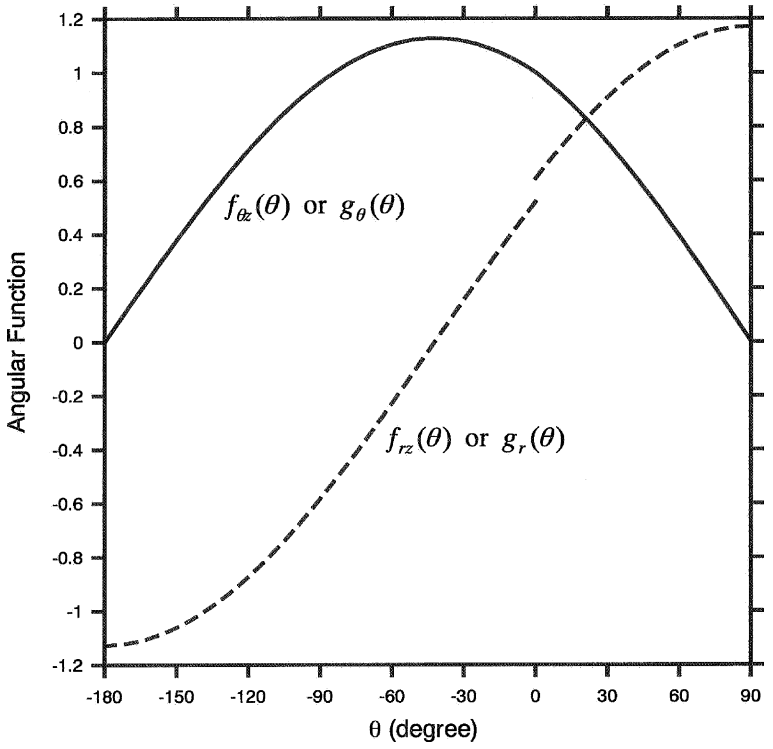

Fig. 4. The variations of the angular functions of the PZT-4–PZT-5 bonded wedge with wedge angles $\alpha = 90°$ and $\beta = 180°$ ($\lambda - 1 = -0.347478$).

3.2.2. Case (2): Complex eigenvalues λ

Consider another example of a PZT-4–PZT-19 bonded wedge that the factor $(R_2^2 - 4R_1) = -0.0246464 < 0$. The eigenvalues are complex. Figs. 5 and 6 show the contours of the strongest singularity order of real and imaginary parts, respectively. The variations of the real part are similar to the previous Case (1). The imaginary parts of the singularity order vanish only when $\alpha = \beta$, $\alpha = 0$ and $\beta = 0$.

There is only one independent variable, say $c_2^{(1)}$, left for the eight unknown constants $c_1^{(1)}$ to $c_4^{(2)}$. From Eq. (18), we have:

$$c_1^{(1)} = Mc_2^{(1)}, \quad c_3^{(1)} = Sc_2^{(1)}, \quad c_4^{(1)} = Qc_2^{(1)}, \quad c_1^{(2)} = Mc_2^{(1)}, \quad c_2^{(2)} = Nc_2^{(1)}, \quad c_3^{(2)} = Sc_2^{(1)},$$
$$c_4^{(2)} = Tc_2^{(1)} \tag{30}$$

where the constants S and T are defined as

$$S = MQ, \quad T = NQ \tag{31}$$

Substituting Eq. (30) into Eq. (8), the stresses and the electric displacements become the forms:

$$\tau_{\theta z} = r^{p-1}\{[\cos(q\log r)f_{\theta z}^c + \sin(q\log r)f_{\theta z}^s]K_{\mathrm{Re}}^\sigma + [\cos(q\log r)f_{\theta z}^s - \sin(q\log r)f_{\theta z}^c]K_{\mathrm{Im}}^\sigma\} \tag{32a}$$

$$\tau_{rz} = r^{p-1}\{[\cos(q\log r)f_{rz}^c + \sin(q\log r)f_{rz}^s]K_{\mathrm{Re}}^\sigma + [\cos(q\log r)f_{rz}^s - \sin(q\log r)f_{rz}^c]K_{\mathrm{Im}}^\sigma\} \tag{32b}$$

$$D_\theta = r^{p-1}\{[\cos(q\log r)g_\theta^c + \sin(q\log r)g_\theta^s]K_{\mathrm{Re}}^D + [\cos(q\log r)g_\theta^s - \sin(q\log r)g_\theta^c]K_{\mathrm{Im}}^D\} \tag{32c}$$

$$D_r = r^{p-1}\{[\cos(q\log r)g_r^c + \sin(q\log r)g_r^s]K_{\mathrm{Re}}^D + [\cos(q\log r)g_r^s - \sin(q\log r)g_r^c]K_{\mathrm{Im}}^D\} \tag{32d}$$

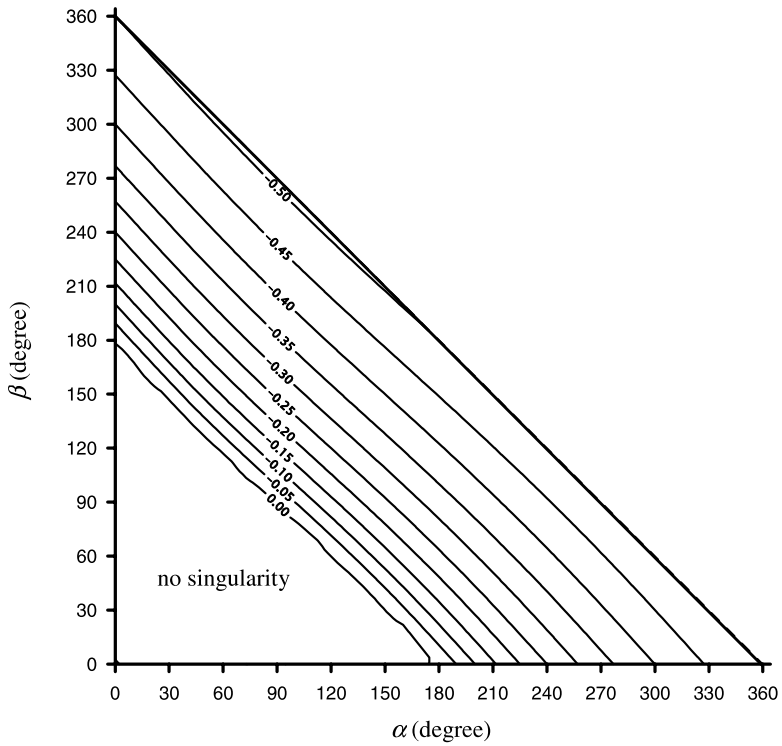

Fig. 5. The variation of the strongest singularity order (real part) of PZT-4–PZT-19 bonded wedges versus the wedge angles α and β.

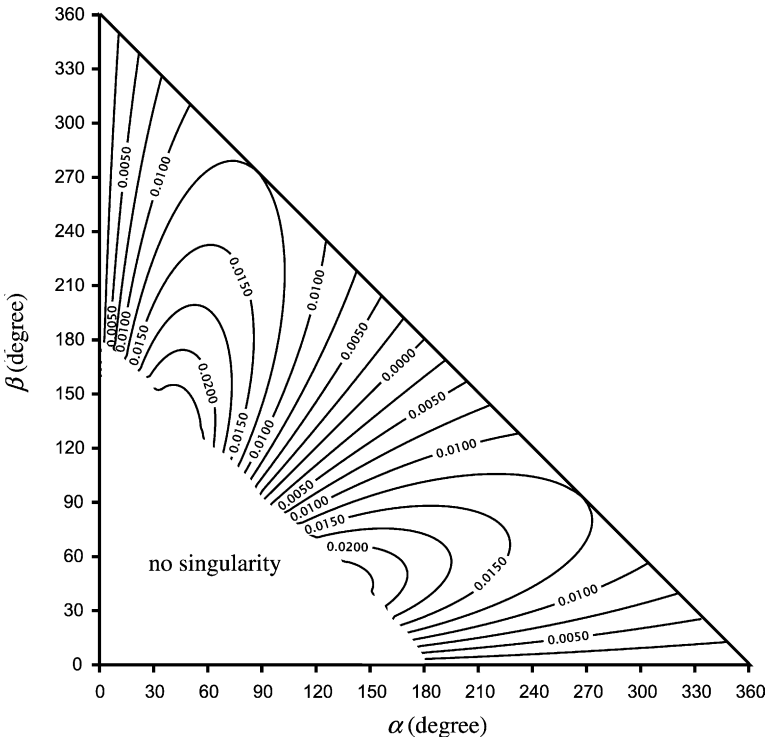

Fig. 6. The variation of the strongest singularity order (imaginary part) of PZT-4–PZT-19 bonded wedges versus the wedge angles α and β.

where p and q are the real and imaginary parts of $\lambda(\lambda = p + \mathrm{i}q)$, respectively. The intensity factors K^{σ}_{Re}, K^{σ}_{Im}, K^{D}_{Re}, and K^{D}_{Im} and angular functions $f^{c}_{\theta z}(\theta)$, $f^{s}_{\theta z}(\theta)$, $f^{c}_{rz}(\theta)$, $f^{s}_{rz}(\theta)$, $g^{c}_{\theta}(\theta)$, $g^{s}_{\theta}(\theta)$, $g^{c}_{r}(\theta)$, and $g^{s}_{r}(\theta)$ are all real-valued. The intensity factors are defined as

$$K^{\sigma}_{\mathrm{Re}} + \mathrm{i}K^{\sigma}_{\mathrm{Im}} = p\mathrm{Re}[C^{(1)}_{44} + e^{(1)}_{15}Q]c^{(1)}_{2} \tag{33a}$$

$$K^{D}_{\mathrm{Re}} + \mathrm{i}K^{D}_{\mathrm{Im}} = \frac{\mathrm{Re}[e^{(1)}_{15} - \varepsilon^{(1)}_{11}Q]}{\mathrm{Re}[C^{(1)}_{44} + e^{(1)}_{15}Q]}(K^{\sigma}_{\mathrm{Re}} + \mathrm{i}K^{\sigma}_{\mathrm{Im}}) \tag{33b}$$

Since $c^{(1)}_{2}$ is an arbitrary complex constant, the generalized stress intensity factors (K^{σ}_{Re}, K^{σ}_{Im}) are two independent variables. Therefore, there are two undetermined and independent constants in the stresses and electric displacements fields. The angular functions in Eq. (32) have the forms:

$$f^{c}_{\theta z} - \mathrm{i}f^{s}_{\theta z} = \begin{cases} \dfrac{\lambda\left(C^{(1)}_{44} + e^{(1)}_{15}Q\right)}{p\mathrm{Re}[C^{(1)}_{44} + e^{(1)}_{15}Q]}\left[\cos(\lambda\theta) - \dfrac{\cos(\lambda\alpha)}{\sin(\lambda\alpha)}\sin(\lambda\theta)\right] & \text{for material 1} \\ \dfrac{\lambda\left(C^{(1)}_{44} + e^{(1)}_{15}Q\right)}{p\mathrm{Re}[C^{(1)}_{44} + e^{(1)}_{15}Q]}\left[\cos(\lambda\theta) + \dfrac{\cos(\lambda\beta)}{\sin(\lambda\beta)}\sin(\lambda\theta)\right] & \text{for material 2} \end{cases} \tag{34a}$$

$$f_{rz}^{c}-\mathrm{i}f_{rz}^{s}=\begin{cases}\dfrac{\lambda\left(C_{44}^{(1)}+e_{15}^{(1)}Q\right)}{p\mathrm{Re}[C_{44}^{(1)}+e_{15}^{(1)}Q]}\left[\sin(\lambda\theta)+\dfrac{\cos(\lambda\alpha)}{\sin(\lambda\alpha)}\cos(\lambda\theta)\right] & \text{for material 1}\\ \dfrac{\lambda\left(C_{44}^{(1)}+e_{15}^{(1)}Q\right)}{p\mathrm{Re}[C_{44}^{(1)}+e_{15}^{(1)}Q]}\left[\sin(\lambda\theta)-\dfrac{\cos(\lambda\beta)}{\sin(\lambda\beta)}\cos(\lambda\theta)\right] & \text{for material 2}\end{cases} \tag{34b}$$

$$g_{\theta}^{c}-\mathrm{i}g_{\theta}^{s}=\begin{cases}\dfrac{\lambda\left(e_{15}^{(1)}-\varepsilon_{11}^{(1)}Q\right)}{p\mathrm{Re}[e_{15}^{(1)}-\varepsilon_{11}^{(1)}Q]}\left[\cos(\lambda\theta)-\dfrac{\cos(\lambda\alpha)}{\sin(\lambda\alpha)}\sin(\lambda\theta)\right] & \text{for material 1}\\ \dfrac{\lambda\left(e_{15}^{(1)}-\varepsilon_{11}^{(1)}Q\right)}{p\mathrm{Re}[e_{15}^{(1)}-\varepsilon_{11}^{(1)}Q]}\left[\cos(\lambda\theta)+\dfrac{\cos(\lambda\beta)}{\sin(\lambda\beta)}\sin(\lambda\theta)\right] & \text{for material 2}\end{cases} \tag{34c}$$

$$g_{r}^{c}-\mathrm{i}g_{r}^{s}=\begin{cases}\dfrac{\lambda\left(e_{15}^{(1)}-\varepsilon_{11}^{(1)}Q\right)}{p\mathrm{Re}[e_{15}^{(1)}-\varepsilon_{11}^{(1)}Q]}\left[\sin(\lambda\theta)+\dfrac{\cos(\lambda\alpha)}{\sin(\lambda\alpha)}\cos(\lambda\theta)\right] & \text{for material 1}\\ \dfrac{\lambda\left(e_{15}^{(1)}-\varepsilon_{11}^{(1)}Q\right)}{p\mathrm{Re}[e_{15}^{(1)}-\varepsilon_{11}^{(1)}Q]}\left[\sin(\lambda\theta)-\dfrac{\cos(\lambda\beta)}{\sin(\lambda\beta)}\cos(\lambda\theta)\right] & \text{for material 2}\end{cases} \tag{34d}$$

It is verified that $f_{\theta z}^{c}(\theta)$, $f_{\theta z}^{s}(\theta)$, $g_{\theta}^{c}(\theta)$ and $g_{\theta}^{s}(\theta)$ are continuous across the interface and vanish at the edges while $f_{rz}^{c}(\theta)$, $f_{rz}^{s}(\theta)$, $g_{r}^{c}(\theta)$ and $g_{r}^{s}(\theta)$ are not.

The formulations derived in this section are based on the assumptions that $\alpha\neq\beta$ and $e_{15}\neq 0$. In the case of $\alpha=\beta$, the characteristic equation (Eq. (24)) and the electro-mechanical field (Eq. (27) for λ is real; Eq. (32) for λ is complex) can be reduced to Eqs. (12) and (16) discussed in Section 3.1 by using the perturbation method. Similarly, using the perturbation method to the case of $e_{15}=0$, the characteristic equation (Eq. (24)) and the electro-mechanical fields (Eq. (32)) derived in this section can be reduced to the following characteristic equation

$$C_{44}^{(1)}\sin(\lambda\alpha)\cos(\lambda\beta)+C_{44}^{(2)}\cos(\lambda\alpha)\sin(\lambda\beta)=0 \tag{35a}$$

$$\varepsilon_{11}^{(1)}\sin(\lambda\alpha)\cos(\lambda\beta)+\varepsilon_{11}^{(2)}\cos(\lambda\alpha)\sin(\lambda\beta)=0 \tag{35b}$$

and the decoupled electro-mechanical field

$$\tau_{\theta z}=K^{\sigma}r^{\lambda-1}f_{\theta z}(\theta) \tag{36a}$$

$$\tau_{rz}=K^{\sigma}r^{\lambda-1}f_{rz}(\theta) \tag{36b}$$

$$D_{\theta}=K^{D}r^{\lambda-1}g_{\theta}(\theta) \tag{37a}$$

$$D_{r}=K^{D}r^{\lambda-1}g_{r}(\theta) \tag{37b}$$

where the angular functions $f_{iz}(\theta)$ and $g_{i}(\theta)$, $i=r,\ \theta$, have the same forms in Eqs. (28) and (29). The characteristic equation (Eq. (35)) and the stress field (Eq. (36)) are identical to the results derived by Ma and Hour (1989). The procedures of the proof are lengthy and will not be stated in this paper.

4. Conclusions

In this paper, the explicit forms of singular electro-mechanical field for a piezoelectric bonded wedge subjected to antiplane shear have been derived analytically. Because of the piezoelectric effect, the singular behavior is different from that of an elastic bonded wedge. The conclusions are summarized as follows:

1. The singularity order of a piezoelectric bi-material bonded wedge is always complex if the following three conditions hold simultaneously: (a) A_1 and A_2 are both complex; (b) $\alpha \neq \beta$; and (c) both α and β are non-zero. If at least one condition does not hold, the singularity order is real. It is quite different from an elastic bonded wedge, in which the antiplane singularity orders are always real.
2. If $\alpha = \beta$, the singularity order is always real. In addition, the eigenvalue is a double-root and the rank of the characteristic matrix $[M]$ is 6. Therefore, there are two independent intensity factors (K^{σ} and K^{D}) in the electro-mechanical field. The present solutions are compared well with the case of an interface crack between two piezoelectric materials.
3. Since the rank of the characteristic matrix $[M]$ is 7 for $\alpha \neq \beta$, the stress and electrical displacement intensity factors are dependent on each other.
4. The electro-mechanical field of case $\alpha \neq \beta$ can be reduced to the cases of $\alpha = \beta$ and/or $e_{15} = 0$ by using the perturbation method. When $e_{15} = 0$, the wedge is decoupled into the electrical and mechanical fields. The results are exactly the same as the antiplane singular field of an isotropic bonded wedge.

Acknowledgement

The authors are grateful to the National Science Council of the ROC for financial support under the contract NSC91-2212-E-006-077.

References

Berlincourt, D.A., Curran, D.R., Jaffe, H., 1964. Piezoelectric and piezoceramic materials and their function in transducers. In: Mason, W.P. (Ed.), Physical Acoustics, vol. I-A. Academic Press, New York.

Bogy, D.B., 1968. Edge-bonded dissimilar orthogonal elastic wedges under normal and shear loading. ASME Journal of Applied Mechanics 35, 460–466.

Bogy, D.B., 1971. Two edge-bonded elastic wedges of different materials and wedge angles under surface tractions. ASME Journal of Applied Mechanics 38, 377–386.

Chen, D.H., Nisitani, H., 1992. Singular stress field in two bonded wedges. Transaction of Japan Society of Mechanical Engineering A 58, 457–464.

Chen, D.H., Nisitani, H., 1993. Singular stress field near the corner of jointed dissimilar materials. ASME Journal of Applied Mechanics 60, 607–613.

Chue, C.H., Chen, C.D., 2003. Antiplane stress singularities in a bonded bimaterial piezoelectric wedge. Archive of Applied Mechanics 72, 673–685.

Chue, C.H., Chen, C.D., 2002. Decoupled formulation of piezoelectric elasticity under generalized plane deformation and its application to wedge problems. International Journal of Solids and Structures 39, 3131–3158.

Dempsey, J.P., Sinclair, G.B., 1979. On the stress singularities in the plane elasticity of the composite wedge. Journal of Elasticity 9, 373–391.

Gandhi, M.V., Thompson, B.S., 1992. Smart Materials and Structures. Chapman and Hall, UK.

Li, X.F., Fan, T.Y., 2000. Semi-infinite anti-plane crack in a piezoelectric material. International Journal of Fracture 102, L55–L60.

Ma, C.C., Hour, B.L., 1989. Analysis of dissimilar anisotropic wedges subjected to antiplane shear deformation. International Journal of Solids and Structures 25, 1295–1309.

Munz, D., Yang, Y.Y., 1993. Stress near the edge of bonded dissimilar materials described by two stress intensity factors. International Journal of Fracture 60, 169–177.

Pak, Y.E., 1990. Crack extension force in a piezoelectric material. ASME Journal of Applied Mechanics 57, 647–653.
Parton, V.Z., Kudryavtsev, B.A., 1988. Electromagnetoelasticity. Gordon and Breach Science Publishers, New York.
Theocaris, P.S., 1974. The order of singularity at a multi-wedge corner of a composite plate. International Journal of Engineering Science 12, 107–120.
Uchino, K., 1997. Piezoelectric Actuators and Ultrasonic Motors. Kluwer Academic Publishers, Norwell Massachusetts.
Xu, X.L., Rajapakse, R.K.N.D., 2000. On singularities in composite piezoelectric wedges and junctions. International Journal of Solids and Structures 37, 3253–3275.